Electrochemical Membrane Flue-Gas Desulfurization: K_2SO_4/V_2O_5 Electrolyte

Douglas S. Schmidt and Jack Winnick
School of Chemical Engineering, Georgia Institute of Technology, Atlanta, GA 30332

The viability of a new electrolyte was demonstrated in the bench-scale electrochemical removal of SO_x from flue-gas streams at high temperatures. At current densities up to 20 A/m^2, approximately 99% current efficiency was achieved when removing 90% of inlet SO_x at 480°C. As current densities increased to 100 A/m^2, current efficiencies were 64% at 480°C and 73% at 520°C. While species present in this K_2SO_4/V_2O_5 molten salt are not well understood, a simple mechanism was used to develop a model to describe the observed removal results. This model was then used to predict preliminary economic viability of this system based on known electrochemical technology.

Introduction

Pollution control has become increasingly stringent with the passage of the Clean Air Act Amendments (40 CFR 61, 1991) by the U.S. Congress in 1990. Included in the pollutants being regulated are sulfur oxides (SO_x), produced primarily in coal-burning power plants. Coal-burning power plants produce approximately 55% of current U.S. power (Smith, 1997), and, with 274-billion-ton estimated recoverable U.S. coal reserves (Bronskowski, 1997), coal will continue to play a prominent role in U.S. power generation.

First-generation postcombustion techniques for removal of SO_x from flue gases generally use a chemically reacting slurry, forming a sludge that must be handled by landfill or through reclamation processes. Second-generation processes such as the SNOX and NOXSO systems are equipment intensive and include complex controls with vapor–liquid separations. Although a salable byproduct, sulfuric acid, is produced by these processes, they have not yet been fully implemented (Borio and Kingston, 1992).

A bench-scale electrochemical-membrane removal system has been developed. It would selectively remove (Winnick, 1990) the dilute SO_3, about 3,000 ppm in a 500 MW power plant burning 3.5% S sulfur coal, from the gas stream at flue-gas temperatures, without heating or cooling cycles. Figure 1 shows conceptual implementation of this system in a coal-burning power plant. Similar in design to the molten carbonate fuel cell (MCFC) shown in Figure 2, this one-step process would also produce, as a result of this selective removal, SO_3, which can be used in the production of a high-purity salable sulfuric acid.

Background

Townley (Townley and Winnick, 1981, 1983; Townley, 1981) first described an electrochemical membrane removal system that used an entrained (Li, K, $Na)_2SO_4$ electrolyte [m.p. 513°C (Lovering and Gale, 1983)] at 550°C. The process used an overall cathodic reaction of

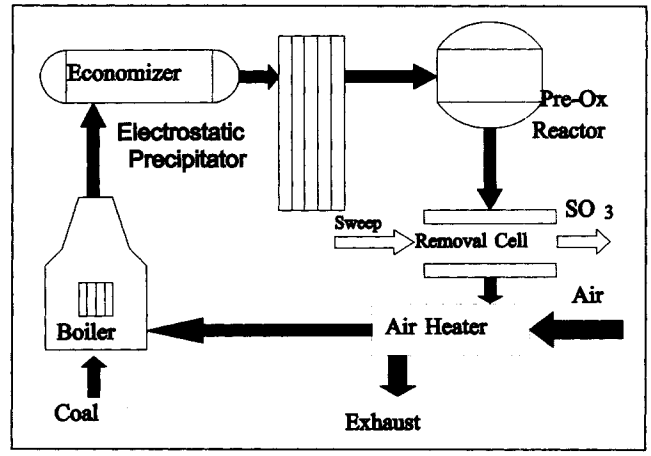

Figure 1. Conceptual implementation of electrochemical removal cell in coal-burning power plant.

Correspondence concerning this article should be addressed to J. Winnick.
Current address of D. S. Schmidt: Westinghouse Science and Technology Center, 1310 Beulah Road, Pittsburgh, PA 15235.

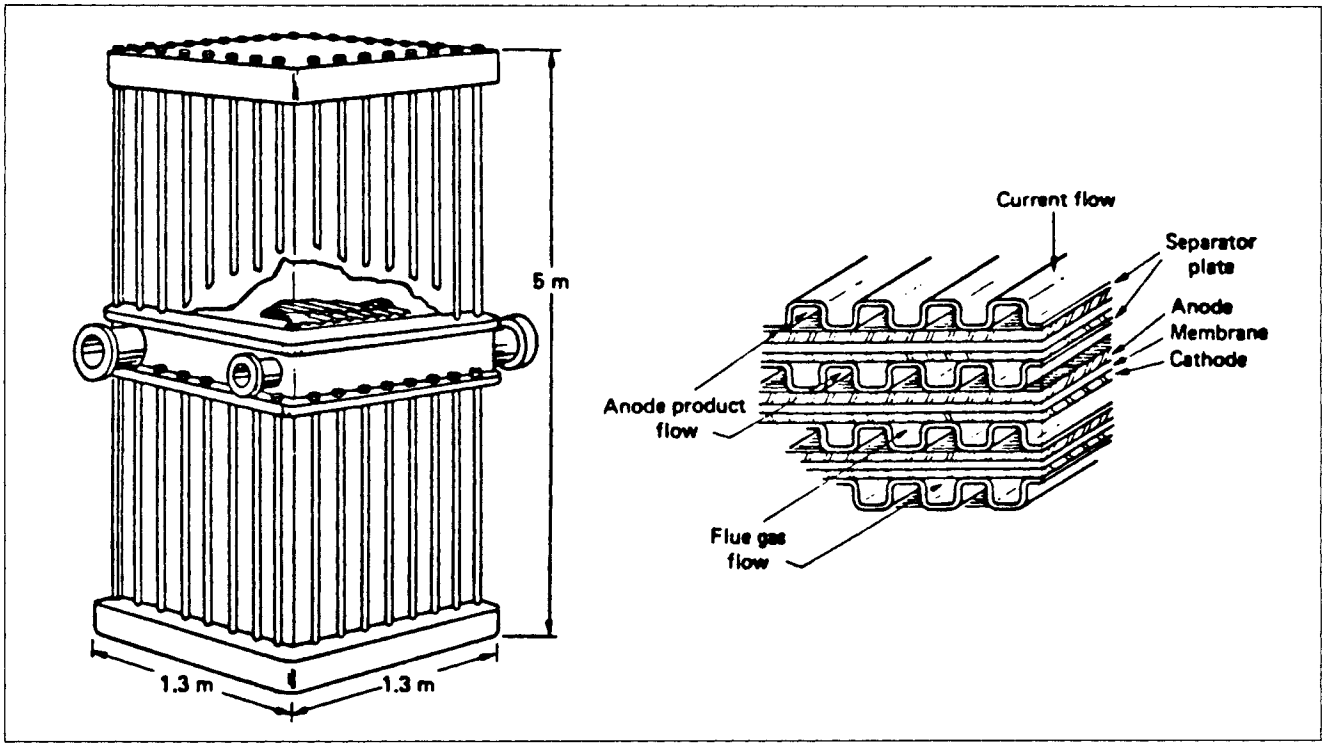

Figure 2. Commercial MCFC with cutaway showing gas flow channels with electrodes and membrane.

$$SO_2 + O_2 + 2e^- \rightarrow SO_4^{2-}, \quad (1)$$

where the SO_2 in the flue gas was reacted at a porous cathode electrode along with oxygen to form sulfate in the molten ternary salt. The flux of SO_x, N_{SO_x}, is directly related to the current density, i, by the stoichiometric relation

$$N_{SO_x} = \frac{i}{2F}. \quad (2)$$

The sulfate was then transported by the electric field through the molten salt to the porous anode electrode where the oxidation was found to be

$$SO_4^{2-} \rightarrow 2e^- + \frac{1}{2}O_2 + SO_3, \quad (3)$$

producing a high-purity oleum. The overall membrane removal process is shown in Figure 3. Townley and Wilemski and coworkers (1979) both showed mass transfer was limited by bulk film diffusion of the dilute species to the porous electrode; transport in the pores of the electrode and through the membrane contributed negligible resistance. However, Townley's system operated at temperatures (550–600°C) far above flue gas temperatures (350–450°C), detrimental to the economics of the system.

Scott (Scott et al., 1988; Scott, 1985) attacked this economic limitation by identifying a new molten salt, a mixture

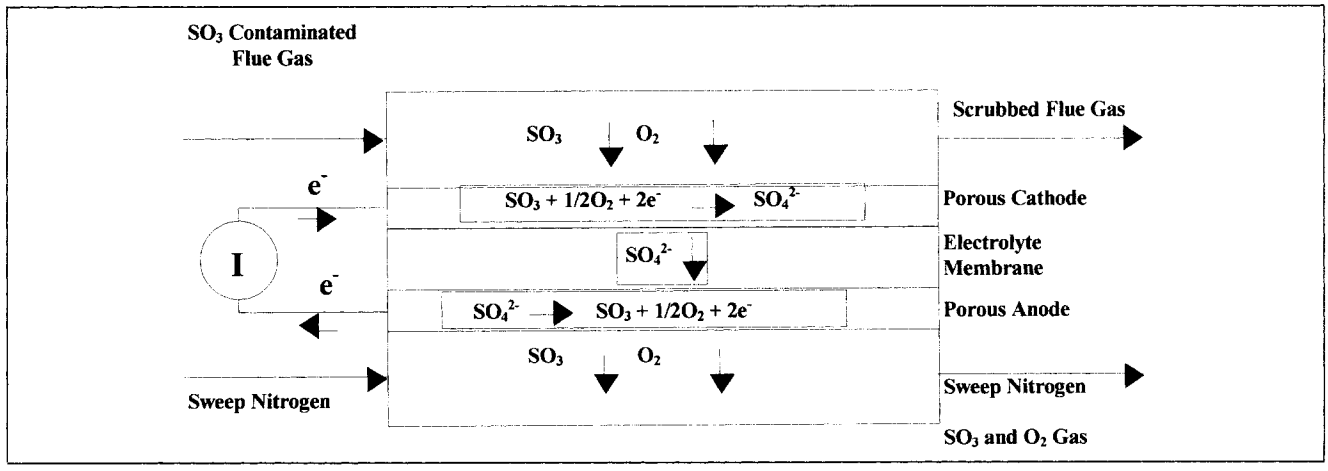

Figure 3. Electrochemical concentration cell describing desired overall reactions.

of pyrosulfate ($K_2S_2O_7$) and vanadium pentoxide (V_2O_5). Potassium pyrosulfate has a melting point of 412°C (Hansen et al., 1982) which can be further depressed with V_2O_5. Franke (Franke and Winnick, 1987, 1989) deciphered the reactions with this melt, showing

$$(SO_2 + O_2)_{\text{cathode}} \xrightarrow{i} \left(SO_3 + \frac{1}{2}O_2\right)_{\text{anode}} \tag{4}$$

as the overall reaction, with vanadia playing a significant role. With pyrosulfate, the primary reduction was of the bulk pyrosulfate

$$2S_2O_7^{2-} + 2e^- \rightarrow SO_2 + 3SO_4^{2-}, \tag{5}$$

resulting in the *production* of SO_2. Sulfur dioxide was oxidized to SO_3 by the oxygen present in flue-gas streams, catalyzed by the V_2O_5 present. This SO_3 combines with SO_4^{2-} to reform pyrosulfate

$$SO_3 + SO_4^{2-} \rightarrow S_2O_7^{2-}. \tag{6}$$

Franke (1988) also showed the presence of a reduction involving vanadia

$$[K_2O \cdot V_2O_5 \cdot 4SO_3] + 2e^- \rightarrow [K_2O \cdot V_2O_4 \cdot 3SO_3] + SO_4^{2-}, \tag{7}$$

although this was not found to affect performance. Franke (1988) and Barzova (Barzova et al., 1971) also described two equilibria in vanadia/pyrosulfate as

$$[K_2O \cdot V_2O_4 \cdot 3SO_3] + \frac{1}{2}O_2 \leftrightharpoons [K_2O \cdot V_2O_5 \cdot 2SO_3] + SO_3 \tag{8}$$

and

$$[K_2O \cdot V_2O_5 \cdot 2SO_3] + 2SO_3 \leftrightharpoons [K_2O \cdot V_2O_5 \cdot 4SO_3], \tag{9}$$

respectively.

McHenry (McHenry and Winnick, 1994) utilized the system description of Franke and identified stable electrode and support components: lithiated nickel oxide (Li_xNi_yO) electrodes and a Si_3N_4 membrane matrix used to support the molten salt. He also initiated use of a preoxidation reactor, oxidizing most SO_2 in the gas stream to SO_3 prior to exposure to the electrochemical system, improving performance by decreasing in-cell vanadia requirements. Using the gas exiting the preoxidation reactor, the overall cathodic reaction in the electrochemical cell became

$$SO_3 + \frac{1}{2}O_2 + 2e^- \rightarrow SO_4^{2-}. \tag{10}$$

As current densities were increased toward economically viable levels of 250 A/m^2, the new phenomena of SO_2 generation at the cathode was observed.

Experimental verification of inlet and outlet gases led to the conclusion that this SO_2 was being generated within the cell, and only with the application of current; when current was removed, SO_3 removal and SO_2 generation ceased. In the removal mechanism of Reaction 5, the reduction of pyrosulfate will produce SO_2. If this electrochemically generated SO_2 is not converted by the vanadium present to SO_3, the removal mechanism is disrupted, resulting in SO_2 evolution at the cathode. In addition, because this generated SO_2 is not oxidized to SO_3, regeneration of pyrosulfate from the combination of sulfate and sulfur trioxide, Reaction 6 will not occur increasing sulfate content at the cathode. As sulfate has a limited solubility of about 4 mol % in pyrosulfate at 412°C (Hansen et al., 1982), electrolyte freezing can potentially exacerbate this problem.

In sulfate melts like that of Townley, removal via an oxide mechanism has been shown by other authors (Salzano and Newman, 1972; Park and Rapp, 1986; Johnson and Laitinen, 1963). The mechanism proposed by these authors was simpler than that of the pyrosulfate system; generally a "direct" reduction of SO_x was observed, considered to be due to an oxide mechanism. Oxygen was first reduced

$$\frac{1}{2}O_2 + 2e^- \rightarrow O^{2-}. \tag{11}$$

The oxide produced electrochemically then combines with SO_3

$$SO_3 + O^{2-} \rightarrow SO_4^{2-}, \tag{12}$$

yielding an overall reaction identical to Reaction 10. This reaction sequence is not as complex as the removal mechanism found in pyrosulfate-based molten salts, and is advantageous for that reason; however, the high melting point of pure sulfates limits this use.

A new molten sulfate mixture is explored in this work, which is a 55 mol % K_2SO_4/45 mol % V_2O_5 sulfate eutectic. This mixture was identified by Boreskov (Boreskov et al., 1954) and Hahle (Hahle and Meisel, 1971) to have a melting point of 430°C and 455°C, respectively, and might offer the advantage of a simple removal mechanism found in other molten sulfates. As no known studies of the constituents of this melt have been reported, the chemistry of the systems presented above was used to provide some insight to this new melt. The new molten salt was tested in this electrochemical removal system to determine its effect on SO_2 generation as well as its effectiveness in SO_x transport.

Experiments

Bench-scale studies (full cell) were conducted using two identical SS316 housings. Each cylindrical housing had milled into it an inlet and outlet flow channel, which allowed gas to flow over a circular electrode well. The flow channel in each housing had a cross-sectional flow area of 0.12×10^{-4} m^2, contacting a superficial electrode area of 20×10^{-4} m^2. Porous gas diffusion electrodes were placed into the elec-

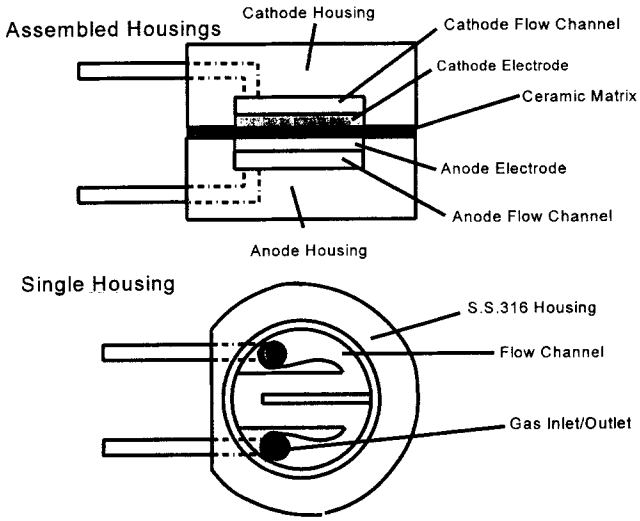

Figure 4. Bench-scale housing used in full-cell testing of electrochemical membrane removal system.

trode well in each housing, and the housings were sandwiched together with the electrochemical molten salt membrane sandwiched in between. This configuration is displayed in Figure 4.

The electrodes were required to be conductive at high temperatures, as well as chemically and electrochemically inert. Their porous nature allowed intimate contact, high interfacial surface area, between the electrode, gas, and electrolyte, necessary for electrochemical removal, placing mass-transfer limitations in bulk film diffusion to the electrode surface as previously discussed. Both the cathode and anode porous gas-diffusion electrodes in these experiments were lithiated nickel oxide (Li_xNi_yO) (McHenry and Winnick, 1994). A 0.001-m-thick 86% porous nickel Fibrex sheet (National Standard) was cut to a cylinder of 0.051 m diameter, providing an area of 20×10^{-4} m^2, and soaked in 1 M LiOH solution for 20 min. It was then simultaneously lithiated and oxidized in air at 600°C for 24 h, resulting in a black, conductive electrode with room-temperature point resistance consistently between 0.3 and 1.2 Ω.

The electrochemical molten-salt membrane consisted of two parts: a supporting porous ceramic matrix and the K_2SO_4/V_2O_5 molten salt. The ceramic matrix supported and stabilized the molten salt at operating temperatures and insulated the cathode from the anode. In addition, the molten salt entrained in the porous ceramic structure formed a wet seal between the cathode and anode sides of the cell, as well as an external wet seal. Phillips Petroleum SN-P Si_3N_4 (courtesy Lyle Kallenbach, Phillips Petroleum) was the ceramic used, as it was found to be stable in this corrosive environment. The membrane used in these experiments was formed by hot pressing 1.00 kg 55 mol % K_2SO_4/45 mol % V_2O_5 with every 1.07 kg Si_3N_4 to form a cylindrical membrane of 0.18×10^{-2} m thickness and area of 45.6×10^{-4} m^2. This membrane, after cooling, was incorporated directly as shown into the cell when assembled.

The entire full-cell assembly was placed into a custom furnace in which temperature was controlled to ±2°C by a Barber-Coleman controller with double-pole relay. A custom blend (Matheson) of 3000 ppm SO_2/3.0% O_2/N_2 was used, as well as N_2 high-purity gas (Air Products). Other contaminant gases such as HCl were not tested; CO_2, H_2O, and NO_x (N_2O, NO, and NO_2) have been found to pass through unchanged (Scott et al., 1988; Townley and Winnick, 1981; McHenry and Winnick, 1994). SO_x was therefore the gas of interest for this study. Gas flow rate was controlled by Matheson 600, 601 and 602 flowmeters, and cathode and anode gases were separately regulated. SO_x measurement was performed by sampling known gas volumes in conjunction with ion chromatography (Driscoll, 1974). SO_2 levels were determined by HP5840A GC with FPD detection. SO_3 was determined by the difference.

Gases to the cathode were first passed through a preoxidation reactor, loaded with Haldor-Topsoe VK-38 sulfuric acid catalyst, at a controlled temperature and of sufficient size to oxidize all SO_2 to SO_3 using available oxygen. At all flow rates used, except for $2{,}000\times10^{-6}$ m^3/min, SO_2 bypass was undetectable. In these initial bench-scale studies, particulates were not introduced. However, the catalyst bed will act as an efficient particulate scrubber (Eggerstedt, 1995; Haas and Olivo, 1994).

Power to the membrane was controlled galvanostatically by a PAR EG&G 371 Potentiostat/Galvanostat. Potentials were monitored by Simpson 460 series multimeters, and ohmic polarization was measured via current interrupt method while it is monitored by a Tecktronix 5111A analog storage oscilloscope.

Results

The primary purpose of this study was the bench-scale verification of SO_x removal using this new system. The data presented here first show the results of the SO_2 generation analysis, followed by process stream SO_x, removal results. All tests were performed with gaseous inlet streams composed of only SO_x, O_2, and N_2.

SO_2 generation

Because SO_2 generation was a problem with a pyrosulfate electrolyte, levels were monitored with current application at both 480°C and 520°C. Figure 5 shows the results with applied current at 480°C for a flow rate of 540×10^{-6} m^3/min and at 520°C for a flow rate of $2{,}000\times10^{-6}$ m^3/min. Generation was calculated as the difference between outlet SO_2 and inlet SO_2. At 480°C, the rate of generation was reduced to approximately 30% of that previously (McHenry and Winnick, 1994) observed with a pyrosulfate mechanism. SO_2 generation was observed to virtually disappear at 520°C, with observed SO_2 levels attributed solely to the unoxidized portion passing through the preoxidation reactor at the highest flow rate. Because these generation levels at 480°C and 520°C were so far below that observed using a pyrosulfate electrolyte, it was apparent that the SO_2 production mechanism prevalent in pyrosulfate was virtually eliminated. Studies therefore concentrated on total SO_x removal only.

SO_x removal

Total SO_x removal was generally tested under two conditions. The first was with no current applied; the second was

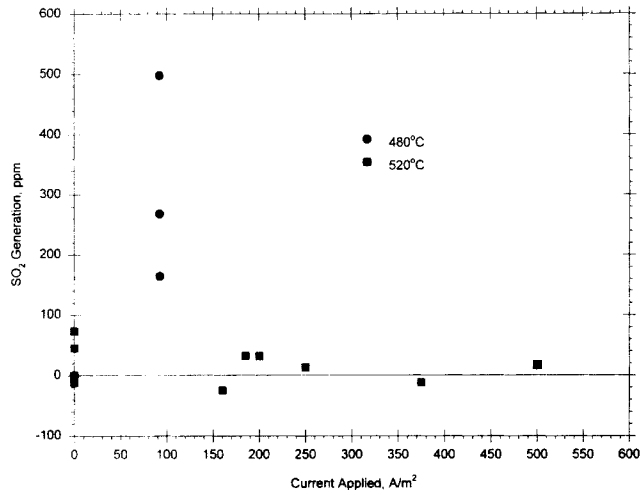

Figure 5. Cathodic SO_2 generation in full-cell testing at 480°C and 540×10^{-6} m^3/min, and 520°C and $2{,}000\times10^{-6}$ m^3/min.

Applied current was calculated as the difference between measured outlet and inlet SO_2; line denotes trend.

with a 90% stoichiometric current density, calculated as

$$i_{90\%} = 90\% \times \frac{\text{(Volumetric flow rate)}}{A_s} \times \frac{P_{SO_3}}{RT} \times nF \quad (13)$$

and based on the superficial electrode area, A_s. Trials were repeated, resulting in replication at 100 A/m^2 and multiple-zero current points for other trials.

Figure 6 shows a typical cathodic response of the system to current application. The lines in these figures are discussed in the next section. These data represent steady state as determined by no change in removal levels over a period of 2 h. It is apparent that some removal is occurring without current; this indicates that some chemical mechanism is functioning. Also important, the application of current enhances the removal, and removal with 90% stoichiometric current application does reach 90%. Efficiency at 20 A/m^2 applied current density was calculated using

$$\epsilon(\%) = \frac{\text{Observed removal}}{\text{Predicted stoichiometric removal for applied current}} \times 100\% \quad (14)$$

as $102 \pm 5\%$.

This zero-current removal is a combination of Reactions 8 and 9 presented in the Background section. With some V_2O_4 present in the melt, and under and SO_3 and O_2 atmosphere at the cathode, without current, the reaction proceeds as

$$[K_2O \cdot V_2O_4 \cdot 3SO_3] + SO_3 + \frac{1}{2}O_2 \leftrightharpoons [K_2O \cdot V_2O_5 \cdot 4SO_3]. \quad (15)$$

At the anode, because the purge was pure N_2, this reaction was reversed, resulting in removal and production under zero-current conditions. The processes occurring at the anode were not fully investigated because the cathode was the primary focus of this study.

Steady-state cathodic removal with the application of 90% stoichiometric current was graphed with respect to the applied current and the corresponding flow rate. Figure 7 shows that at low current densities, approximately stoichiometric removal was achieved. Because current density increased to 100 A/m^2, total SO_x removal percentages decreased. Current efficiencies decreased to 67% and removal to 64% at 100 A/m^2 from 102% efficiency and 91% removal at 20 A/m^2. The cell exhibited total electrochemical cell overpotential of 0.9 V at 100 A/m^2, where overpotential is calculated by

$$\eta = E_{\text{total}} - iR, \quad (16)$$

where η is the overpotential, indicative of the required energy for the system, E_{total} is the total cell potential measured

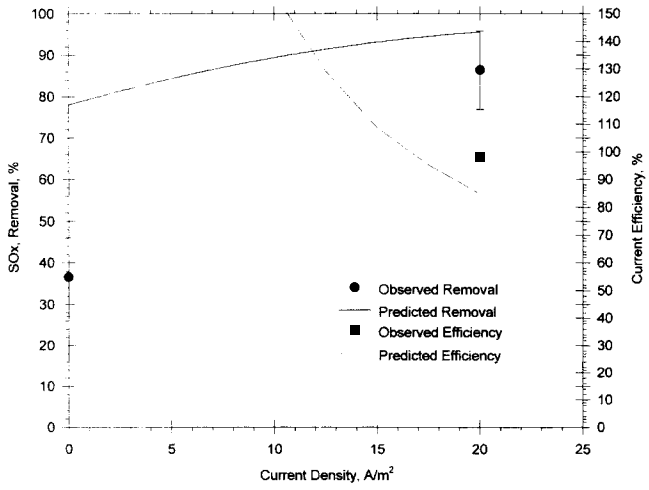

Figure 6. Experimental removal and current efficiency at 90×10^{-6} m^3/min and 480°C.

Lines are calculated using Eqs. 23 and 24.

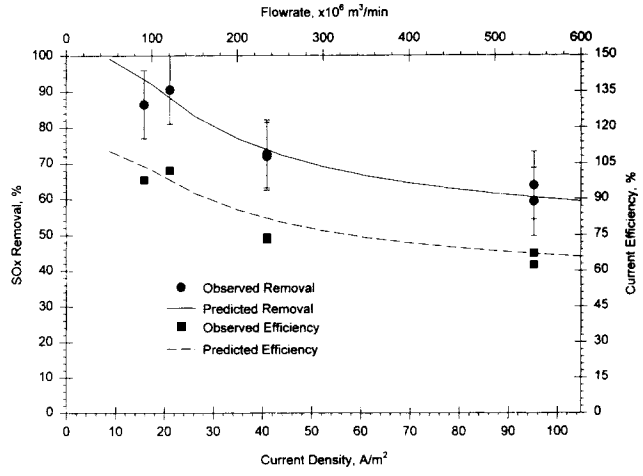

Figure 7. Experimental removal and current efficiency for a 90% stoichiometric current-varying flow rate.

Lines are calculated using Eqs. 23 and 24.

by voltmeter, and iR represents the ohmic or inherent resistance of the cell, a quantity that can be controlled by reducing membrane thickness and external wiring resistances. Additional details of polarization results are found elsewhere (Schmidt et al., 1997b).

To better quantify this response, a simplified model was developed that would describe the SO_x removal process occurring at the cathode, with and without applied current.

SO_x Removal Modeling

The first step in the modeling process was to describe the removal mechanism. Removal of SO_x from the cathode gas stream was the only process considered. For this, a direct oxide mechanism was assumed to exist. Although the actual process involves more complex chemical species (Schmidt et al., 1997a), this would allow the main removal sequence to be represented by

$$SO_3(g) + O^{2-}(l) \rightarrow SO_4^{2-}(l), \tag{17}$$

with oxide production from current occurring according to

$$\frac{1}{2}O_2 + 2e^- \rightarrow O^{2-}. \tag{18}$$

The oxide shown in this reaction corresponds neither to the $[K_2O \cdot V_2O_5 \cdot 2SO_3]$ nor $[K_2O \cdot V_2O_4 \cdot 3SO_3]$ previously presented, and sulfate is also probably not the exact transport species in this complex system. However, since exact species were not known in this melt, it was assumed that this might suffice in this first modeling attempt, as the overall removal mechanism developed previously was based on an effective oxide mechanism.

Based on Reaction 17, the rate equation for the chemical removal of SO_3 is

$$r_{SO_3} = k_1 P_{SO_3}^{m_0} [O^{2-}]^{m_1} \tag{19}$$

where r_{SO_3} is the flux of SO_3, k_1 is the rate constant, and m_i is the reaction order. The surface concentration of oxide in the system was unknown, and needed to be evaluated for successful implementation of the model.

A mass balance was performed around the system in terms of the differential rate of surface oxide production. Surface oxide produced with current according to Reaction 18 was written stoichiometrically as i/nF. This oxide disappeared either in the reaction desired, previously shown as $-r_{SO_3}$, or through some other reaction of the oxide (reaction with other chemical species, migration from the cathode surface to the anode), which was written as $-k_2\,[O^{2-}]^{m_2}$. Finally, some zero-current removal of SO_3 was observed at the cathode. Reaction 15 suggested that this removal mechanism was dependent on the partial pressure of O_2 at the cathode. Assuming this oxygen involvement is the limiting factor in the rate of zero-current removal, and that the effective surface oxide production was the result of this oxygen involvement, the rate of oxide production was directly linked to the partial pressure of oxygen as $k_3\,p_{O_2}^{m_3}$. Combination of all these terms at steady state led to the equation

$$\frac{d[O^{2-}]}{dt} = 0 = \frac{i}{nF} - r_{SO_3} - k_2[O^{2-}]^{m_2} + k_3 P_{O_2}^{m_3}. \tag{20}$$

At these high temperatures, kinetic rates are high. For this reason and the fact that only limited data were available, all rates were assumed to be first order, setting all $m_i = 1$. This reaction order would be indicative of a mass-transfer-controlled system, where apparent reaction rates are controlled by transport.

Rearrangement of Eq. 20 led to an explicit solution for the surface oxide concentration

$$[O^{2-}] = \frac{\dfrac{i}{nF} + k_3 P_{O_2}}{k_1 P_{SO_3} + k_2}, \tag{21}$$

which could then be substituted back into Eq. 19 to solve for the rate of removal of SO_3 from the process gas

$$r_{SO_3} = k_1 P_{SO_3}\left(\frac{\dfrac{i}{nF} + k_3 P_{O_2}}{k_1 P_{SO_3} + k_2}\right). \tag{22}$$

Equation 22 shows that at zero current, SO_3 removal is due solely to the presence of oxygen. As currents become high, the current accounts for a greater proportion of the total oxide production. In addition, if there are no losses, removal is linear with applied current density at a given temperature and oxygen partial pressure. Equation 22 can be rearranged to only involve two parameters: (k_2/k_1) and k_3:

$$r_{SO_3} = \frac{\dfrac{i}{nF} + k_3 P_{O_2}}{1 + \left(\dfrac{k_2}{k_1}\right)\dfrac{1}{P_{SO_3}}}. \tag{23}$$

Separation of k_2 and k_1 would require additional independent oxide or oxygen data for this particular system; these data were not available, and only one oxygen partial pressure was used throughout these experiments, precluding such an analysis. With two parameters, two data were required to fit the expression.

The model predicts that at high flow rates with no current for a given inlet partial pressure of SO_3 and O_2, the removal rate will be higher than that for lower flow rates, but the percentage removal will be lower at the high flow rates. In addition, the model suggests greater than 100% current efficiencies may be possible due to the chemical removal mechanism.

A logarithmic-mean concentration average was used to represent the concentration in the bulk stream. All flows were at $N_{Re} \leq 100$, and the assumption was made that N_{Sh} was constant over the experimental N_{Re} range. Using experimental data for inlet and outlet concentrations, and knowing the flow rate through the system, the partial pressure of SO_3 at the reaction interface was estimated by

$$r_{SO_3} = k_m\left(C_{SO_3,\text{bulk}} - \frac{P_{SO_3,\text{surface}}}{RT}\right) \qquad (24)$$

where k_m is the mass-transfer coefficient and could be correlated from independent gas-phase correlation (Incropera and DeWitt, 1985), and R and T have their usual significance. The limit due to film mass transfer was calculated based on $N_{Sh} = 5.1$ in this square channel laminar flow geometry. Two data at the same temperature allowed explicit evaluation of the constants k_3 and (k_2/k_1). Because high flow rates and current densities are likely in full-scale systems, the combination of points yielding the least error between prediction and observed values at 100 A/m^2, and the lowest relative overall error were chosen. At 480°C, $k_3 = 5.3\times10^{-3}$ mol/atm/m^2/s and $(k_2/k_1) = 0.00173$ atm were found to meet these two criteria.

The model predicts removal at zero currents, and that this removal, as a percentage, will decrease as flow rate increases, as the system is limited by the chemical removal mechanism. Applied current level increases become important at high flow rates, as the contributions of gas-phase mass transfer and competing reactions increase substantially.

These values were substituted into Eq. 23, and both removal efficiency and percentage removal were predicted for bench-scale flow rates of 90×10^{-6} m^3/min (Figure 6), 120×10^{-6} m^3/min (Figure 8), 232×10^{-6} m^3/min (Figure 9), and 540×10^{-6} m^3/min (Figure 10) at 480°C. These figures show the prediction to be extremely accurate at the higher flow rates, suffering substantially only at the 90×10^{-6} m^3/min flow rate. The model accurately predicted removal levels with 90% applied stoichiometric current density over the range of tested flow rates (Figure 7).

At 520°C, only one set of data was taken at 540×10^{-6} m^3/min. To use the model at this new temperature, an assumption was required, as two points need be used to determine the two parameters at each temperature. Following from the discussion that the reaction orders and rates were controlled by diffusion in the melt, and assuming that the change in the rate constants with temperature would be identical, the ratio of the two rate constants (k_2/k_1) would remain almost constant over the 40°C temperature increase. With this assumption, at 520°C, $k_3 = 9.5\times10^{-3}$ mol/atm/m^2/s was found to best fit the data.

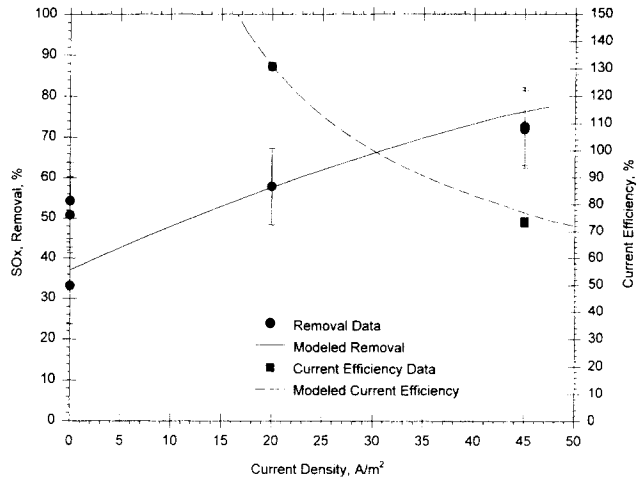

Figure 9. Experimental removal and current efficiency at 232×10^{-6} m^3/min and 480°C.

Lines are calculated using Eqs. 23 and 24.

Figure 11 presents a comparison of the data and model prediction at 480°C and 520°C. Again, the model predicted removal well within the maximum error shown. The increase in removal with temperature may have resulted from faster transport. The higher temperature may also improve the conductivity of the electrolyte. Near the eutectic melting point, very small changes in local concentration may result in electrolyte solidification; at a higher temperature this will not be as likely to occur.

Preliminary Economics

To determine the economic viability of this system in comparison to other systems, a preliminary economic analysis was performed similar to that presented by Franke (Franke and

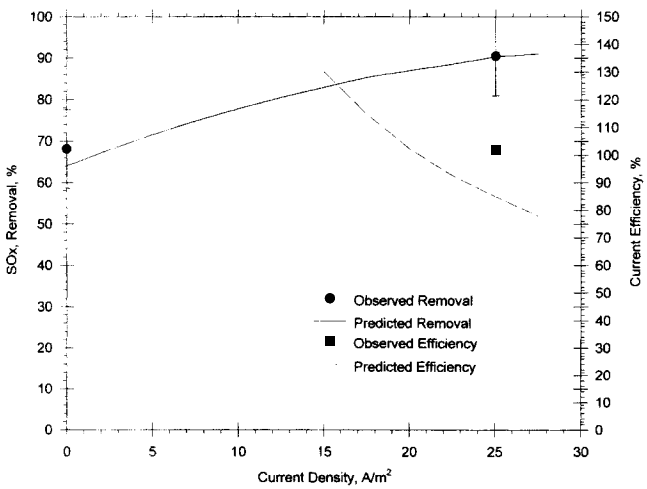

Figure 8. Experimental removal and current efficiency at 120×10^{-6} m^3/min and 480°C.

Lines are calculated using Eqs. 23 and 24.

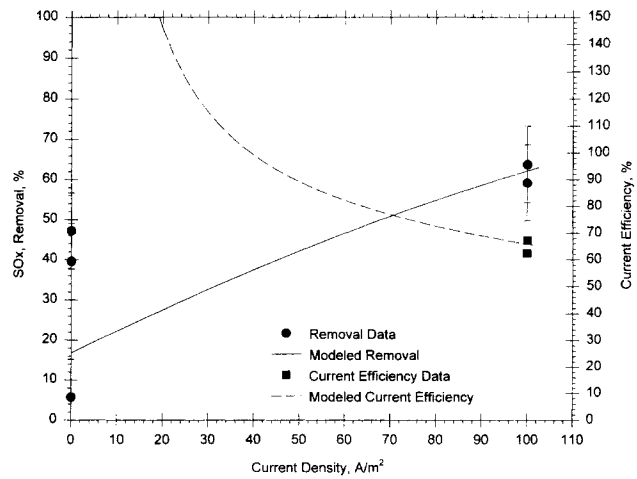

Figure 10. Experimental removal and current efficiency at 540×10^{-6} m^3/min and 480°C.

Lines are calculated using Eqs. 23 and 24.

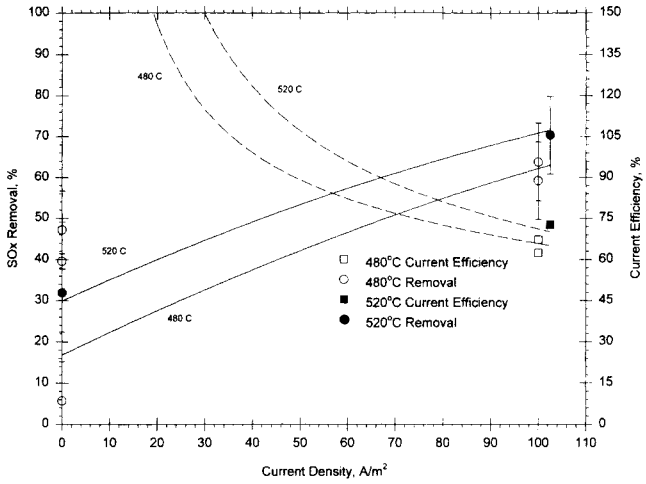

Figure 11. Experimental removal and current efficiency for 540×10^{-6} m³/min at 480°C and 520°C.

Lines are calculated using Eqs. 23 and 24.

Winnick, 1989) and McHenry (McHenry, 1992). Extended details of these calculations are found elsewhere (Schmidt, 1997).

We first assume that the economics and design of a similar electrochemical system, the MCFC, are applicable to a full-scale electrochemical membrane system. Based on an MCFC with 36 m^2 superficial surface area, the costs described by Appleby (Appleby and Foulkes, 1989) were applied on a per area basis.

The primary design parameter was the size of the gas-flow system to ensure optimization of SO_x transport to the membrane for the separation. This parameter was balanced by the need for a low pressure drop and the resulting current density. Costs were based on a 30-year equipment and ten-year electrochemical stack lifetime, and fourth-quarter 1996 dollars.

A 500-MW power plant burning South Illinois coal (Shannon, 1982) with 3.5% S with a boiler efficiency of 35% and 20% excess air produced a stream with about 2,900 ppm SO_2 and 3.5% O_2. To facilitate 90% removal, 53.43 mol SO_2/s must be removed, requiring an area of 113,244 m^2. Operating costs consisted of the cost of electricity, \$0.03/kWh, at an estimated stack voltage of 2 V; this assumes iR is controlled to approximately 1 V. This level of ohmic polarization is far higher than that achieved in the MCFC with similar configuration (Appleby and Foulkes, 1989). A small (\$86/ton) credit was taken for sulfuric acid production. A preoxidation reactor (\$10.6 million) and sulfuric acid production plant (\$9 million) were included in operating and capital costs (McHenry and Winnick, 1994). The low ~ 300 ppm SO_3 outlet projected from this process should not condense in the process, as preheater temperatures of 230°C are well above the dew point of 165°C. (Schoubye, private communication, 1996). It is also assumed that the preoxidation reactor temperature is controlled to optimize SO_2 oxidation for the process. Inflation was assumed to be 5% and a discount factor of 10% was used.

Using the model, an operating current density of 210 A/m^2 (23,781,401 A) using 9.5% plant power was predicted to effect 90% removal with a current efficiency of 43%, resulting in a levelized cost of 7.9 mill/kWh. First generation systems may have a levelized cost of 1.8 to 2.5 times this level (Cooper and Alley, 1994). By comparison, the NOXSO process is listed (Black et al., 1993) as having a levelized cost of 8.5 mill/kWh and the SNOX (Borio et al., 1993) as 7.83 mill/kWh. Because operating costs in this electrochemical removal are dependent on electrical power consumption, if the electrochemical system is optimized based on 100% current efficiency, the levelized cost drops to 4.9 mill/kWh.

It is important to note that the equipment-intensive SNOX and NOXSO processes economize on scale and sulfur content. If power plants become smaller and localized as predicted by the Department of Energy (U.S. Department of Energy, 1992), this more modular electrochemical membrane removal system will become far more desirable.

Conclusions

A new bench scale K_2SO_4/V_2O_5 molten salt electrochemical membrane system was tested for use in removing SO_x from flue gas in coal-burning power plants. At 20 A/m^2, 90% removal was shown with approximately 99% current efficiency at 480°C. As the current density was increased to 100 A/m^2, 65% removal was shown at 63% current efficiency at 480°C and 72% removal with 67% current efficiency at 520°C.

For the first time, a model was developed using simple engineering principles to describe the removal and current efficiency in this process. This model was then used to determine the economic viability of the system.

Preliminary analysis showed that even at current performance levels, this technology is economically competitive in a 500-MW plant. However, due to the modular design of the system, the electrochemical membrane system should compete well in smaller power plants. To improve the process, specific identification of the reactions occurring is needed. However, with a modicum of improvement in efficiency, costs, already lower than first-generation removal systems, should decrease substantially.

Acknowledgment

The authors recognize the support of the Department of Energy under Grant DE-FG22-90PC90293.

Notation

C_i = concentration of component i, mol/m^3
F = Faraday's constant, 96,501 C/Eq
N_{Sh} = Sherwood number
N_{Re} = Reynolds number
n = number of electrons in reaction, eq/mol
P_i = partial pressure of component i, atm
R = gas constant, 8.314 J/mol/K
T = temperature, K
$[O^{2-}]$ = surface oxide concentration, mol/m^2

Literature Cited

Appleby, A. J., and F. R. Foulkes, *Fuel Cell Handbook*, Van Nostrand Reinhold, New York (1989).

Barzova, Z. G., G. K. Borenskov, A. A. Ivanov, L. G. Karakchiev, and L. D. Kockina, "Study of the V_2O_5-$K_2S_2O_7$ System Under Conditions for Oxidation of Sulfur Dioxide," *Kinet. Katal. (USSR)*, **12**, 948 (1971).

Black, J. B., M. C. Woods, J. J. Friedrich, and C. A. Leonard, "The NOXSO Clean Coal Technology Project: Commercial Plant Design," Annu. Clean Coal Technology Conf., Atlanta, GA (1993).

Boreskov, G. K., V. V. Illarionov, R. P. Ozerov, and E. V. Kildisheva, "Chemical Reactions in Vanadium Pentoxide-Potassium Sulfate and Vanadium Pentoxide-Potassium Pyrosulfate Systems," *J. Gen. Chem. (USSR)*, **24**, 21 (1954).

Borio, R. C., and W. H. Kingston, "High Efficiency SO_2 and NO_x Abatement with No Waste Generation–The SNOX Process," *Asea Brown Boveri* (1992).

Borio, D. C., D. J. Collins, and T. D. Cassell, "Performance Results from the 35MW SNOX Demonstration at Ohio's Edison Niles Station," Ann. Clean Coal, "SNOX Demonstration Project: 1. Public Design," Dept. of Energy, Final Report, DE-FC22-90PC89655 (1996).

Bronskowski, R., *U.S. Coal Reserves: A Review and Update, Executive Summary*, Department of Energy, Washington, DC, p. 1 (1997).

Cooper, C. D., and F. C. Alley, *Air Pollution Control: A Design Approach*, Waveland Press, Prospect Heights, IL, p. 482 (1994).

Driscoll, J. N., *Flue Gas Monitoring Techniques*, Ann Arbor Science, Ann Arbor, MI (1974).

Eggerstedt, P. M., "Simultaneous Hot Desulfurization and Improved Filtration in Coal Utilization Processes," Dept. of Energy, Washington, DC, p. *DOE/METC-95/1081*, Vol. I, 342 (1995).

40 CFR 61, Code of Federal Regulations, Title 40, Part 61, *Emission Standards for Hazardous Air Pollutants*, Office of Federal Register, Washington, DC (1991).

Franke, M., "Electrochemical Flue Gas Clean-Up," PhD Diss., Georgia Inst. of Technol., Atlanta (1988).

Franke, M., and J. Winnick, "The Electrochemistry of Molten $K_2S_2O_7 + K_2SO_4 + V_2O_5$ Electrolytes," *J. Electroanal. Chem.*, **238**, 163 (1987).

Franke, M., and J. Winnick, "Membrane Separation of Sulfur Oxides from Hot Gas," *Ind. Eng. Chem. Res.*, **28**, 1352 (1989).

Haas, J. C., and C. A. Olivo, "Multi-Contaminant Control Granular Bed Filter," Dept. of Energy, Washington, DC, *DOE/METC-94/1008*, Vol. I, p. 176 (1994).

Hahle, S., and A. Meisel, "Phase Analysis of the Active Component of Vanadium Catalysts Containing Potassium," *Kinet. Katal.*, **12**, 1276 (1971).

Hansen, N. H., R. Fehrmann, and N. J. Bjerrum, "Complex Formation in Pyrosulfate Melts: 1. Potentiometric, Cyroscopic, and Spectrophotometric Investigations of the Systems $K_2S_2O_7$-K_2SO_4 and $K_2S_2O_7$-K_2SO_4-V_2O_5 in the Temperature Range 410-450°C," *Inorg. Chem.*, **21**, 744 (1982).

Incropera, F. D., and D. P. DeWitt, *Fundamentals of Heat and Mass Transfer*, 2nd ed., Wiley, New York, p. 398 (1985).

Johnson, K. E., and H. A. Laitinen, "Electrochemistry and Reactions in Molten Li_2SO_4-Na_2SO_4-K_2SO_4," *J. Electrochem. Soc.*, **110**, 314 (1963).

Lovering, D. G., and R. J. Gale, *Molten Salt Techniques*, Vol. 1, Plenum Press, New York, p. 115 (1983).

McHenry, D. J., "Development of and Electrochemical Membrane Process for Removal of SO_x/NO_x from Flue Gas," PhD Diss., Georgia Inst. of Technol., Atlanta (1992).

McHenry, D. J., and J. Winnick, "Electrochemical Membrane Process for Flue Gas Desulfurization," *AIChE J.*, **40**, 143 (1994).

Park, C. O., and R. A. Rapp, "Electrochemical Reactions in Molten Na_2SO_4 at 900°C," *J. Electrochem. Soc.*, **133**, 1636 (1986).

Salzano, F. J., and L. Newman, "Sulfur Trioxide, Oxygen, Platinum Electrode in a Fused Sulfate," *J. Electrochem. Soc.*, **119**, 1273 (1972).

Schmidt, D. S., "Electrochemical Removal of SO_x from Flue Gas," PhD Diss., Georgia Inst. of Technol., Atlanta (1997).

Schmidt, D. S., J. Winnick, R. Fehrmann, and S. Boghosian, "Electrochemical and Spectroscopic Investigations of the K_2SO_4-V_2O_5 Molten Electrolyte," *J. Electrochem. Soc.*, in press (1997a).

Schmidt, D. S., D. J. McHenry, and J. Winnick, "Lithiated Nickel Oxide Electrode Performance in Molten $K_2S_2O_7/V_2O_5$ and K_2SO_4/V_2O_5 Systems," *J. Electrochem. Soc.*, in press (1997b).

Scott, K., "Electrochemical Flue-Gas Desulfurization," PhD Diss., Georgia Inst. of Technol., Atlanta (1985).

Scott, K., T. Fannon, and J. Winnick, "Electrochemical Flue Gas Desulfurization," *J. Electrochem. Soc.*, **135**, 573 (1988).

Shannon, R. H., *Handbook of Coal-Based Electric Power Generation*, Noyes, New Jersey, p. 165 (1982).

Smith, S., *Electric Power Monthly—February 1997 Monthly Update, Executive Summary*, Dept. of Energy, Washington, DC, p. 1 (1997).

"SNOX Demonstration Project: 1. Public Design," Dept. of Energy, Final Report, DE-FC22-90PC89655 (1996).

Townley, D., "Electrochemical Concentration of Sulfur Oxides from Flue Gas," PhD Diss., Georgia Inst. of Technol., Atlanta (1981).

Townley, D., and J. Winnick, "Electrochemical Sulfur Dioxide Concentration for Flue-Gas Desulfurization," *Electrochim. Acta*, **28**, 389 (1983).

Townley, D., and J. Winnick, "Flue Gas Desulfurization Using an Electrochemical Sulfur Oxide Concentrator," *Ind. Eng. Chem. Proc. Des. Dev.*, **20**, 435 (1981).

U.S. Department of Energy, *Clean Coal Technology: The New Coal Era*, DOE/FR-0217P, Washington, DC (1992).

Wilemski, G., T. Wolf, D. Bloomfield, M. L. Finson, E. R. Pugh, and K. L. Wray, "Performance Model for Molten Carbonate Fuel Cells," DE-AC-03-79ET11322, U.S. Department of Energy, Washington, DC (1979).

Winnick, J., "Electrochemical Membrane Gas Separation," *Chem. Eng. Prog.*, **86**(1), 41 (Jan. 1990).

Manuscript received Apr. 28, 1997, and revision received Sept. 18, 1997.